

# High-efficiency switching effect in porphyrin-ethyne-benzene conjugates

Yi-Peng An,<sup>1</sup> Zhongqin Yang,<sup>1,2,a)</sup> and Mark A. Ratner<sup>2</sup>

<sup>1</sup>State Key Laboratory of Surface Physics and Department of Physics, Fudan University, Shanghai 200433, China

<sup>2</sup>Department of Chemistry, Northwestern University, Evanston, Illinois 60208, USA

(Received 25 April 2011; accepted 4 July 2011; published online 27 July 2011)

We have explored the electronic transport properties of porphyrin-ethyne-benzene conjugates using an *ab initio* method. The results indicate that these ethyne-bridged phenyl porphyrin molecules can be used as candidates for molecular switching devices. The coplanar conformation of phenyl and porphyrin moieties allows a far larger current than the perpendicular conformation due to the near vanishing overlap of the frontier molecular orbitals ( $\pi$  channels) in the porphyrin and phenyl parts in the latter. Higher current ratios of ON/OFF states can be obtained if amino or nitro substituent is placed at the position meta to the bridge connecting the  $\pi$  systems of the molecule. The substituent group affects the electronic state energy of the entire molecule in coplanar conformation, while only affecting the local part in perpendicular conformation. More complex ethyne-bridged diphenyl porphyrin molecules are found to yield more complex and interesting switching effects. Our results suggest that such molecular wires composed of appropriate  $\pi$ -conjugated molecules, can generally display perfect switching function and the efficiency can be tuned flexibly by adding certain substituent groups to the conjugates. © 2011 American Institute of Physics. [doi:10.1063/1.3615492]

## I. INTRODUCTION

Miniaturization of traditional electronic devices remains as a prime target for electronics. Under this trend, molecular electronics has become a diverse and rapidly growing field. In recent years, there have been several suggestions for electronic devices at the molecular or atomic scale both in theoretical proposals and experimental reports.<sup>1–10</sup> Several molecules have been discovered with striking functional properties, such as negative differential resistance (NDR) behavior,<sup>11</sup> spin filter,<sup>12</sup> rectification,<sup>13</sup> field-effect transistors,<sup>14</sup> and switching behaviors,<sup>15–17</sup> etc. It is of significance to explore such sensitive electronic transport behaviors of molecules, which may be employed in the design of future molecular devices.

Several organic molecules or nanowires show novel functional properties based on the  $\pi$  systems. These include  $\pi$ -conjugated ring molecules, such as the simplest arene molecules,<sup>18,19</sup> porphyrin molecules<sup>20,21</sup> that have good chemical stability, rigid planar geometry, and highly conjugated structure, or some of their conjugates.<sup>16,22–24</sup> Their special geometries lead to extensive interest in the application to molecular devices. Organic molecules are typically not very rigid, and the bonds can flex and bend. Moresco *et al.*<sup>16</sup> reported a detailed experimental and theoretical investigation of electronic transport properties of the complicated Cu-tetra-3,5 di-ter-butyl-phenyl porphyrin (Cu-TBPP) molecules. Upon rotating one TBP leg induced by the scanning tunneling microscope tip, the Cu-TBPP molecule shows strong switching behavior. Ghosh *et al.*<sup>25</sup> explored the field-effect mechanisms of benzene-based molecular devices through twisting the intramolecular conformation by a gate electrode. With

advanced laser techniques, researchers can more easily manipulate the torsion of some conjugated molecules by laser pulses.<sup>26</sup> These may provide ultrafast molecular switches in future nanoelectronics applications. Here, using the first-principles technique we explore the electronic transport properties of some porphyrin-ethyne-benzene conjugates which have different intramolecular conformations. Switching with high ON/OFF ratios can be achieved, and the corresponding mechanisms will be analyzed.

## II. COMPUTATIONAL METHODS

The structure optimizations of all the isolated porphyrin-ethyne-benzene conjugates investigated in this report were performed in advance using the plane-wave generalized gradient approximation (GGA) method implemented in the Vienna *ab initio* package.<sup>27</sup> The optimized molecules were then chemisorbed (terminal hydrogen atoms removed) at the fcc sites of two (4 × 4)(111) gold surfaces. The height of the S atom above the surface was fixed to 2.00 Å, which is close to the equilibrium Au-S bond length suggested in the literature.<sup>28</sup> Then their electronic transport properties were explored using the Atomistix ToolKit software package.<sup>5–7</sup> As shown in Fig. 1(a) for the sample porphyrin-ethyne-benzene molecule junction, in practical theoretical simulations, such a two-probe system is divided into three parts: The left and right electrodes, which contains three (4 × 4)(111) Au layers, respectively, and the central scattering region containing the molecule and four surface layers of electrode in total. The properties of the left and right electrode regions are obtained from a calculation with periodic boundary conditions in all directions. The region between the two electrodes is described with open boundary conditions in the transport direction and periodic boundary conditions in the

<sup>a)</sup>Electronic mail: zyang@fudan.edu.cn.

directions perpendicular to the transport direction. For all these two-probe systems, the nonlocal norm-conserving Troullier–Martins pseudopotentials<sup>29</sup> are used to describe the core electrons for all atoms, and valence electrons are expanded in single- $\zeta$  plus polarization basis sets for Au atom while double- $\zeta$  plus polarization basis sets is used for other atoms to achieve a balance between the calculation efficiency and the accuracy. The exchange–correlation potential is described by the Perdew–Burke–Ernzerhof parametrization of the GGA function. A mesh cutoff of 150 Ry for real-space grid is set and the Monkhorst–Pack  $k$ -points grid  $3 \times 3 \times 100$  is used to sample the Brillouin zone to obtain the accurate results. Test calculations with larger cutoff energy and  $k$ -points grid sampling yield the very similar results. When bias applied, the density matrix of scattering region for this nonequilibrium system, with two different chemical potentials ( $\mu_L$  and  $\mu_R$ ), is constructed by using nonequilibrium Green’s function (NEGF)  $\hat{G}^<$ ,<sup>1,5,7</sup>

$$\hat{\rho} = -\frac{i}{2\pi} \int dE \hat{G}^<(E), \quad (1)$$

where

$$\hat{G}^< = \hat{G}^R \hat{\Sigma}^< [f_L(E - \mu_L), f_R(E - \mu_R)] \hat{G}^A \quad (2)$$

and  $\hat{G}^{R/A}$  is the retarded/advanced Green’s function of the device,  $f_{L/R}$  is the Fermi–Dirac distribution function of electrode. The quantity  $\hat{\Sigma}^< [f_L(E - \mu_L), f_R(E - \mu_R)]$  expresses injection of charge from the electrodes and can be written in terms of the self-energies  $\hat{\Sigma}_L$  and  $\hat{\Sigma}_R$  due to coupling to the left and right electrodes,

$$\hat{\Sigma}^< [f_L(E - \mu_L), f_R(E - \mu_R)] = -2i \text{Im} [f_L(E - \mu_L) \hat{\Sigma}_L + f_R(E - \mu_R) \hat{\Sigma}_R]. \quad (3)$$

It is most efficient to obtain the density matrix by using NEGF formalism and avoid calculating the scattering states, although it is equivalent to steady scattering theory.<sup>7</sup> Once the self-consistent solution is obtained, we can evaluate the transmission coefficients,<sup>1</sup>

$$T(E) = \text{Tr} [\hat{\Gamma}_L(E) \hat{G}^R(E) \hat{\Gamma}_R(E) \hat{G}^A(E)], \quad (4)$$

where the broadening function  $\hat{\Gamma}_{L,R} = i[\hat{\Sigma}_{L,R}^R - \hat{\Sigma}_{L,R}^A]$  is given by the self-energies  $\hat{\Sigma}_L$  and  $\hat{\Sigma}_R$ , respectively. Then the current  $I$  through the central molecule can be calculated from Landauer–Büttiker formula,<sup>30</sup>

$$I(V_b) = \frac{2e}{h} \int_{-\infty}^{\infty} T(E) [f_L(E - \mu_L) - f_R(E - \mu_R)] dE. \quad (5)$$

More details of the calculation method can be consulted in previous reports.<sup>1–7</sup> Note that in spite of NEGF formalism used in our calculations, the incoherent and time-dependent effects etc. were not considered. Some deep discussions on these aspects in quantum transport can be found in Ref. 2.

### III. RESULTS AND DISCUSSIONS

Three different kinds of ethyne-bridged phenyl porphyrin conjugates are considered in this report. The coplanar and per-

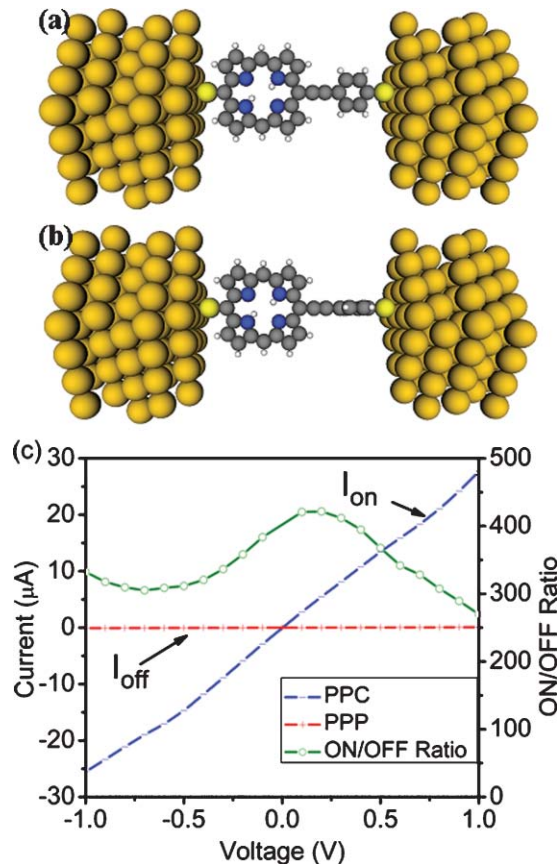


FIG. 1. (a) and (b) for the two intramolecular conformations of porphyrin-ethyne-benzene molecule connected to two semi-infinite  $(4 \times 4)(111)$  gold electrodes using terminal thiol groups. The sulfur atoms are fixed at the fcc sites of two gold surfaces with a perpendicular distance of 2.00 Å (corresponding to an Au-S distance of 2.60 Å). (a) and (b) give the ethyne-bridged PPC and PPP conformations, respectively. (c) shows the  $I$ - $V$  curves for PPC and PPP. The ON/OFF ratio of current as a function of applied voltage is also included.

pendicular intramolecular conformations are our main focus, and the effect of the substituents is also investigated.

#### A. Porphyrin-ethyne-benzene junctions

As shown in Figs. 1(a) and 1(b), we first explored the electronic transport properties of a porphyrin-ethyne-benzene molecule coupled to the Au electrodes. Two isomers are analyzed for this molecule: first with the porphyrin and phenyl rings coplanar (labeled as PPC) and then  $90^\circ$  twisted into the perpendicular (labeled as PPP). For the isolated molecules terminated with thiols, the calculated relative stability of the isomers predicts PPC to be more stable than PPP by 66.7 meV, which is close to that barrier range of 35–90 meV of Bianthrone molecular switch.<sup>31</sup> This implies that it is not difficult to achieve the torsion from coplanar to perpendicular conformation by laser or other techniques<sup>16,25,32,33</sup> due to the proper energy difference. Since the energy difference between PPP and PPC is not much larger than the thermal energy at room temperature, it is the best to carry out the experiments in low temperature to reduce the thermal effect.

The calculated current–voltage ( $I$ – $V$ ) curves of PPC and PPP are given in Fig. 1(c) with the bias voltage varying from  $-1.0$  to  $1.0$  V. It can be seen that the current through PPC increases quickly and almost linearly with the increase of applied voltage, implying that the coplanar conformation can easily pass the current through the circuit. For the perpendicular conformation, the current through PPP is very weak (close to zero). PPP has poor electron tunneling ability, nearly switching the current off. Clearly, in the process of porphyrin-ethyne-benzene molecule twisting from coplanar to perpendicular conformation, the current through the circuit can switch from ON to OFF. Therefore, the ethyne-bridged phenyl porphyrin molecule is a candidate for molecular switching devices. As shown in Fig. 1(c), high ON/OFF ratios of the current (270–420) are achieved under the applied bias voltage from  $-1.0$  to  $1.0$  V. This is far larger than the factor (about 1.2) of bipyridyl-dinitro oligophenylene-ethynylene dithiol<sup>34</sup> and 31 of 4,4'-biphenyl dithiolate molecule.<sup>35</sup>

Molecular conductance generally follows the characteristics of molecular orbitals, particularly the frontier molecular orbitals (highest occupied molecular orbital (HOMO), lowest unoccupied molecular orbital (LUMO)), and the HOMO–LUMO gap. To understand the switching mechanism, we calculate the transmission spectrum and molecular projected self-consistent Hamiltonian (MPSH) (Ref. 36) for HOMO and LUMO energy levels at zero bias for PPC and PPP, respectively. Surprisingly, the transmission probabilities of PPP are very low in the whole energy range considered, even at the energy positions of the HOMO ( $E = -0.46$  eV) and LUMO ( $E = 1.04$  eV), as shown in Fig. 2(a). This behavior arises because the electrons cannot easily tunnel through the junction because of the orthogonality of the  $\pi$  systems in PPP. For PPC, all the characteristics, the larger transmission probability at  $E_F$ , smaller HOMO–LUMO gap (about 1.27 eV) and two sharp transmission peaks near  $E_F$  which originates from the HOMO ( $E = -0.37$  eV) and LUMO ( $E = 0.9$  eV), respectively, indicate that PPC conducts electrons well and can easily keep the circuit in the ON state. The reason for these properties in PPC is that the phenyl and porphyrin  $\pi$  states are not perpendicular to each other. Figures 2(b) and 2(c) give the projected densities of states (PDOSs) of PPC and PPP in the molecular junctions, respectively, and PDOSs on porphyrin and phenyl are also included. The positions of the PDOS peaks near  $E_F$  for both PPC and PPP correspond well to the HOMO and LUMO levels. As shown in Fig. 2(b) for PPC, there are peaks near  $-0.37$  and  $0.9$  eV for both porphyrin and phenyl parts, illustrating strong overlap of states from the both parts in coplanar geometry. In sharp contrast, the HOMO and LUMO of the PPP junction are dominated by the contributions from the porphyrin. The state contributions near  $E_F$  from the phenyl ring move farther away from  $E_F$  when the geometry changes from coplanar to perpendicular conformation. The tunneling electrons are thus blocked due to lack of amplitude on the benzene component in the twisted geometry. This is the reason why an ‘ON’ state appears in PPC case while ‘OFF’ describes the PPP case.

The real-space distributions of HOMO and LUMO of PPC and PPP are given in Fig. 3, which illustrate intuitively the transport behaviors of the two conformations. For PPC,

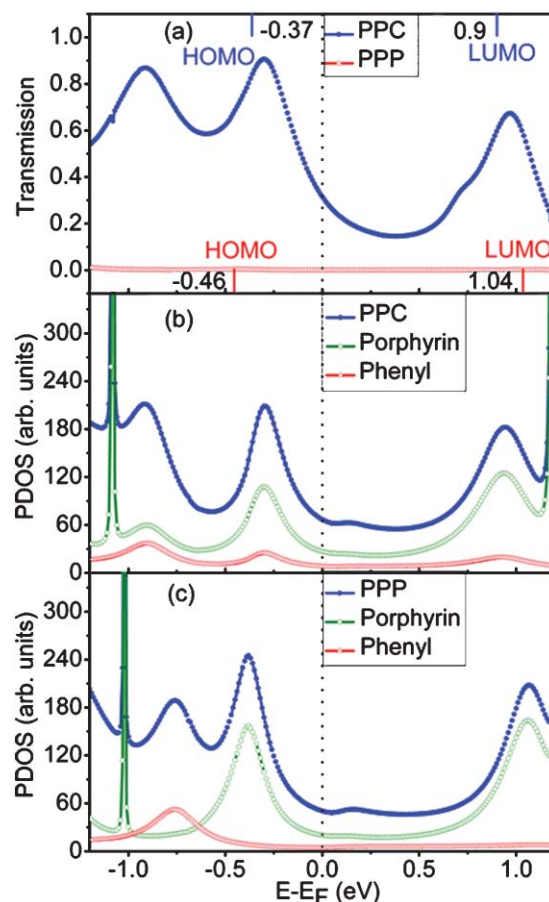


FIG. 2. (a) Transmission spectra, MPSH for HOMO and LUMO energy levels at zero bias voltage for PPC and PPP junctions. (b) PDOSs on porphyrin, phenyl, and the whole PPC molecule. (c) PDOSs on porphyrin, phenyl, and the whole PPP molecule. The Fermi level is set to zero.

both HOMO and LUMO distribute widely not only on porphyrin but also on phenyl. Delocalized  $\pi$  molecular orbitals on the whole PPC molecule significantly contribute to the electron tunneling. For both HOMO and LUMO of PPP, the states localize on porphyrin and there is very small amplitude broadened on phenyl. The extension of the  $\pi$  channels over the porphyrin-ethyne-benzene molecule is broken when the phenyl plane is tuned to the perpendicular conformation. Notice also the substantial  $\pi$ -type charge density on the S atoms: This is seen for *both* S atoms in PPC, but only for *one* in PPP. The choice of threefold coordination for the S/Au interaction allows direct contact with the sulfur  $\pi$  basis function, providing a pathway into the molecular orbitals.<sup>37</sup> When the  $\pi$ -conjugated porphyrin and phenyl rings are in the same plane, the contributing  $\pi$  orbitals will have the maximum overlap to each other and lead to the lowest resistance in the junction. Complete misalignment between the two rings will lead to localization of the frontier orbitals on the porphyrin (and its sulfur) and thus to weaken electron tunneling probability. The smaller PDOS for phenyl in PPP could be due to the longer  $\pi$  system in porphyrin than in phenyl.

As stated in previous reports,<sup>16,25,26,32,33</sup> several techniques might be used to control the intramolecular conformation, such as the laser control, gate electrode effect,

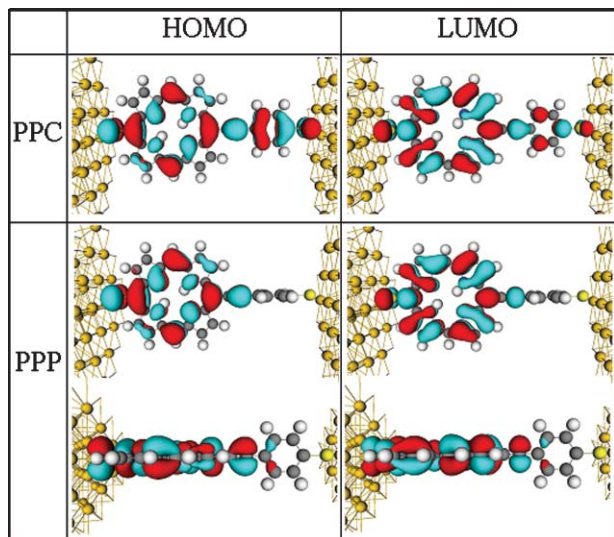


FIG. 3. MPSH eigenstates of the HOMO and LUMO of PPC and PPP at zero bias voltage. Both the top and vertical views are given for PPP. The isovalue of molecular orbitals is  $0.05 \text{ \AA}^{-3/2}$ . The red/blue color expresses the positive/negative wavefunction.

bulky substituents, bridging structures, and self-assembly techniques, etc. Our DFT calculations show that PPC has lower energy (about 66.7 meV) than PPP, which can be easily understood by using the free electron model for the systems.<sup>38</sup> Thus, this porphyrin-ethyne-benzene molecular switch is naturally inclined to its coplanar conformation, leaving the switch on the ON state. Like the laser control switch 3,5-difluor-3', 5'-dibromo-biphenyl,<sup>26</sup> it is believed that when an appropriate laser pulse train acts on the phenyl (or porphyrin) part and twists it to perpendicular conformation, the current through the circuit drops sharply and the OFF function of the switch is achieved. In addition, by tuning the direction and changing the speed of the laser pulses or fixing the laser pulses for long time at proper position,<sup>32</sup> the phenyl (or porphyrin) may be forced to rotate quickly around the C-C bond axis. As a result, this molecular switch will change between PPC and PPP conformations time and again. A special switch with alternative ON or OFF state can be achieved. Therefore, the porphyrin-ethyne-benzene molecule may be a candidate for ultrafast molecular switches with high efficiency.

## B. Influence of substituent groups

Since the electronic properties of molecular junction can be modified strongly by adding functional group such as amino, nitro, etc. to the molecules, some novel behaviors such as NDR or switching can be obtained and utilized.<sup>39,40</sup> Herein, we explore the electronic transport properties of amino-substituted and nitro-substituted porphyrin-ethyne-benzene molecules.

The models of two conformations of ethyne-bridged phenyl porphyrin substituent at the position ortho to the sulfur with amino (PPA) molecular junctions, namely, the coplanar conformation of phenyl and porphyrin rings (PPAC)

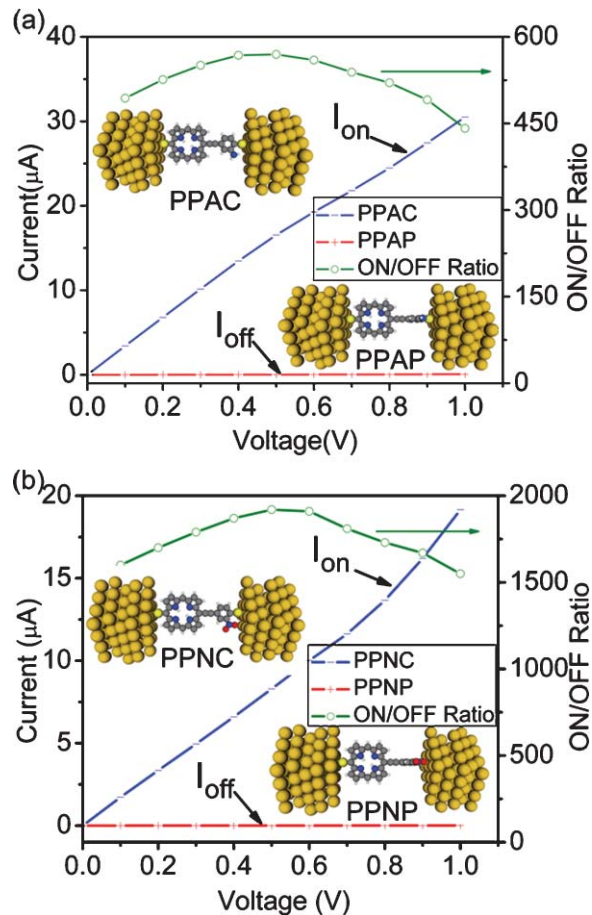


FIG. 4. The  $I$ - $V$  curves and ON/OFF ratio of the current for PPA (a) and PPN (b) molecular junctions with their two conformations.

and its perpendicular conformation (PPAP), are shown in Fig. 4(a). From the  $I$ - $V$  curves of PPAC and PPAP, one sees that the switching behavior can again be achieved by twisting the porphyrin or phenyl-amino part from coplanar to perpendicular conformation. The ON/OFF ratio ( $\sim 550$ ) for the PPA molecule is higher than that ( $\sim 350$ ) of the ethyne-bridged phenyl porphyrin molecule. The corresponding results of ethyne-bridged phenyl porphyrin substituted with nitro (PPN) junctions are given in Fig. 4(b), where PPNC and PPNP express the corresponding coplanar and perpendicular conformations of phenyl and porphyrin rings, respectively. The PPN molecular switch has a much higher switching ratio (near 2000) than those of the ethyne-bridged phenyl porphyrin and PPA molecules.

Generally, amino ( $\text{NH}_2$ ) and nitro ( $\text{NO}_2$ ) groups have opposite electron withdrawing capability: the former tends to lose electrons and the latter to gain. Why are the switching ratios induced by the two groups not opposite but both increased? To understand the electronic transport behaviors of the two kinds of molecular junctions, we plot and analyze their transmission spectrum and MPSH eigenvalues of the HOMO and LUMO in Figs. 5(a) and 5(d), respectively. In comparison with those of ethyne-bridged phenyl porphyrin molecular junctions, the transmission spectra of PPAC and PPAP (Fig. 5(a)) display similar trends, but with larger

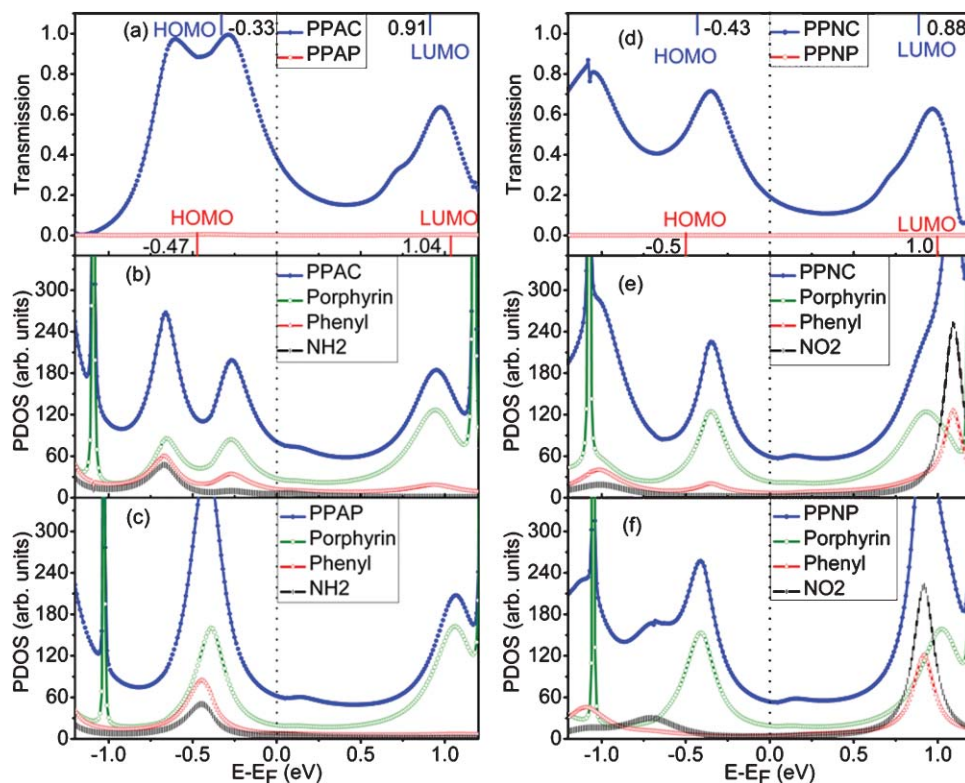


FIG. 5. (a) Transmission spectra and projected HOMO and LUMO levels for PPA molecular junctions with different conformations (PPAC and PPAP). (b) and (c) PDOSs on porphyrin, phenyl, amino, and the whole molecule in separated PPAC and PPAP junctions. (d), (e), and (f) are the same as (a), (b), and (c), except for PPN molecular junctions instead. The  $E_F$  is set to zero.

magnitude for PPAC than PPC near  $E_F$ . The amino substitution makes the HOMO ( $E = -0.33$  eV) of PPAC closer to  $E_F$  and more able to transmit electrons.

Adding a nitro group gives rise to lower transmission in PPNC junction (Fig. 5(d)), compared to PPAC or PPC cases. The HOMO of PPNC, which is nearer to  $E_F$  than the LUMO, goes away from  $E_F$  slightly in PPC (see Figs. 5(d) and 2(a)). This explains why the nitro group slightly reduces the transmission of the junctions with PPC. Similar to Fig. 2(b), both porphyrin and phenyl contribute to the HOMO levels in PPAC ( $-0.33$  eV) and PPNC ( $-0.43$  eV), with large components from porphyrin (see Figs. 5(b) and 5(e)). In comparison with the position of HOMO in PPC ( $-0.37$  eV), the shift of the HOMO level in PPAC and PPNC can be rationalized well by the electron-loss behavior of  $\text{NH}_2$  group and electron-gain of  $\text{NO}_2$  group.

When the conformations between porphyrin and phenyl are changed from coplanar to perpendicular, the influence of the substituted groups is different. From Figs. 2(c), 5(c), and 5(f), one can see that the PDOSs of porphyrin in the three molecular junctions do not vary much, with the almost same shapes and peak-positions. The PDOSs of phenyl in the three cases, however, change much. From PPNP, PPP, to PPAP the PDOS peak of the valence state of phenyl moves towards  $E_F$  gradually (from  $-1.1$ ,  $-0.75$  to  $-0.4$  eV). This trend can be explained by the fact that in perpendicular conformation, the substituted group, attached to phenyl, affects phenyl part. The porphyrin part changes very slightly due

to weak overlap of the electronic states at the porphyrin and phenyl interface. The influence of the substituted group changes from the entire sample molecule to only the phenyl part when the conformation varies from coplanar to perpendicular. Due to the small and large relative misalignment of the energy levels of porphyrin and phenyl in PPAP and PPNP (Figs. 5(c) and 5(f)), the transmissions of PPAP and PPNP increase and decrease, respectively, at zero bias, compared to PPP. (The trend can be seen when the Figs. 2(a), 5(a), and 5(d) are enlarged.) Additionally, compared to PPP, the transmission of PPAP cannot increase much because of the very low amplitude of the HOMO level on the phenyl group. This causes the ON/OFF ratio in current to increase slightly after amino is added. For PPNP, the large misalignment of the energy levels of porphyrin and phenyl in Fig. 5(f) makes the efficiency of the electron tunneling very low, illustrating the reason why the nitro group induces so large ON/OFF ratio ( $\sim 2000$ ) in porphyrin-phenyl molecular junction. Thus, both amino and nitro groups can tune the switching effect of ethyne-bridged phenyl porphyrin molecule. The nitro group can provide extremely high efficiency.

### C. Ethyne-bridged diphenyl porphyrin molecular junctions

As stated above, when these molecules have reduced  $\pi$  overlap and thus strong localization of molecular orbitals on one of the rings, the electron tunneling channels will be

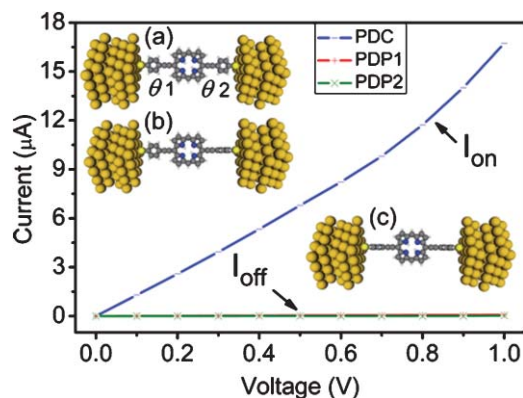


FIG. 6. The  $I$ - $V$  curves for ethyne-bridged diphenyl porphyrin molecular junctions with three different kinds of intramolecular conformations: (a) PDC, (b) PDP1, and (c) PDP2. ' $\theta_1$ ' in (a) expresses the angle between the planes of the left phenyl and porphyrin; ' $\theta_2$ ', the angle between the planes of the porphyrin and the right phenyl.

blocked; the circuit is in an OFF state. To verify this switching mechanism, we further explored the case of triad ethyne-bridged diphenyl porphyrin molecule. As illustrated in Fig. 6, here we investigated three intramolecular conformations: (a) all rings are coplanar (PDC) with the  $\theta_1 = 0^\circ$  and  $\theta_2 = 0^\circ$ , labeled as  $(0^\circ, 0^\circ)$ ; (b) one phenyl is perpendicular to the other (PDP1) with  $(0^\circ, 90^\circ)$ ; and (c) porphyrin is perpendicular to two phenyls (PDP2) with  $(90^\circ, 90^\circ)$ .

The  $I$ - $V$  curves of these junctions with the three kinds of intramolecular conformations are shown in Fig. 6. The PDC can let the current pass. Both PDP1 and PDP2 display low electron tunneling probability, with the circuit in the OFF state. The calculated average ON/OFF ratio of PDC/PDP1 is about 200, and more exciting ON/OFF ratio of PDC/PDP2 is about 4000. The reason can be illustrated well by the MPSH eigenstates in Fig. 7. The perfect extension of  $\pi$  channels over the coplanar conformation is broken when one phenyl is perpendicular to others (PDP1). When the central stronger  $\pi$ -conjugated portion porphyrin is twisted to the conformation perpendicular to the original plane, the  $\pi$  frontier orbitals localize on porphyrin (PDP2). The frontier molecular orbitals for PDP1 and PDP2 show small amplitude on phenyl parts. As shown in Fig. 7, the state localization is much stronger in PDP2, causing the larger ON/OFF ratio of PDC/PDP2 than in PDC/PDP1. Considering the symmetry of the molecule, one can adopt three feasible techniques to achieve the switching function from ON to OFF states, namely, twisting the left phenyl, right phenyl, or central porphyrin to the perpendicular conformation through laser pulse control<sup>26</sup> or other probe techniques.<sup>16,25,32,33</sup> Therefore, a multi-strategy approach to a molecular switch is suggested.

To further explore the role of porphyrin in the multi-strategy molecular switch, we investigated the following models: (a) changing the angle  $\theta_1$  between the porphyrin and the left phenyl in PDP1 from  $0^\circ$  to  $15^\circ$ ,  $30^\circ$ , ...; and (b) removing the porphyrin from PDP1 to obtain the Au-S-phenyl-C<sub>4</sub>-phenyl-S-Au junction (labeled as PCPP), as shown in Fig. 8(a). We see that with the increase of the angle  $\theta_1$  the molecular conductance increases first, and then decreases. The current is the largest when the porphyrin has the same

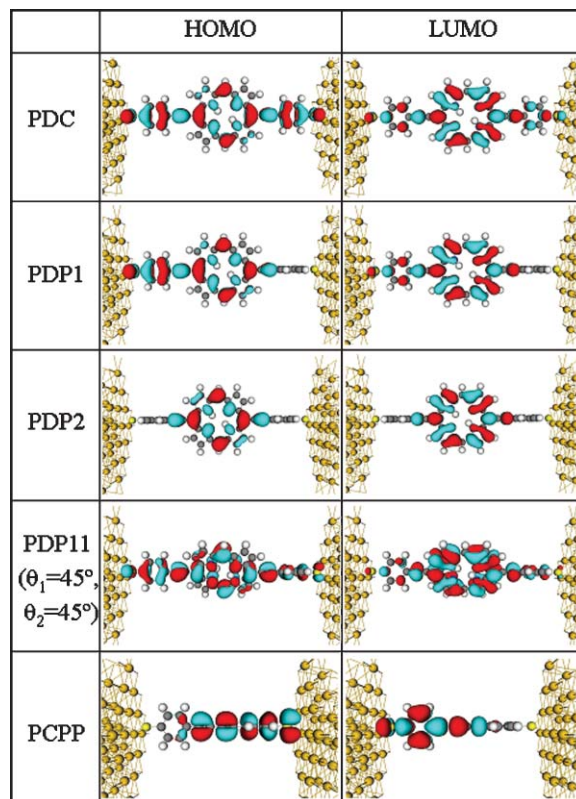


FIG. 7. MPSH eigenstates of HOMO and LUMO at zero bias, for the junctions of PDC, PDP1, PDP2, PDP11 (with the angles of  $(45^\circ, 45^\circ)$ ), and PCPP, respectively.

angle  $\theta$  (equals to  $45^\circ$ ) with the two phenyls since the effective overlap of molecular orbitals between porphyrin and the phenyls (left and right) is still good (see PDP11 in Fig. 7). The result of maximum current for the geometry of  $(45^\circ, 45^\circ)$  indicates that the transmission of those molecular junctions is primarily determined by the subunit overlap of the wavefunctions between different parts. Near perpendicularity destroys overlap and therefore leads to very small transmission in the junction, such as the case with the angles of  $(0^\circ, 90^\circ)$  in Fig. 8. One more special property appears when the transmission of PDP11 ( $45^\circ, 45^\circ$ ) is compared to that of PCPP. Although the length of molecular wire for the former is longer, the molecular transmission is much larger in the former. This is interesting because the two benzenes in both cases are perpendicular. In spite of the small interaction between the two benzenes in PCPP, there is considerable interaction between the two benzenes in PDP11 due to the bridging porphyrin between them with the angle of  $45^\circ$ , rationalized well through perturbation theory.<sup>41,42</sup> Thus, a super exchange behavior is working for PDP11 ( $45^\circ, 45^\circ$ ) junction to induce the large transmission, while there is no such scheme for PCPP junction. This mechanism provides a way to increase the conductance of conjugated molecules in perpendicular conformation. By controlling the intramolecular conformations of porphyrin-ethyne-benzene conjugates, some other electronic transport behaviors such as triangular or rectangular<sup>32</sup> current may also be expected in these molecular wires.

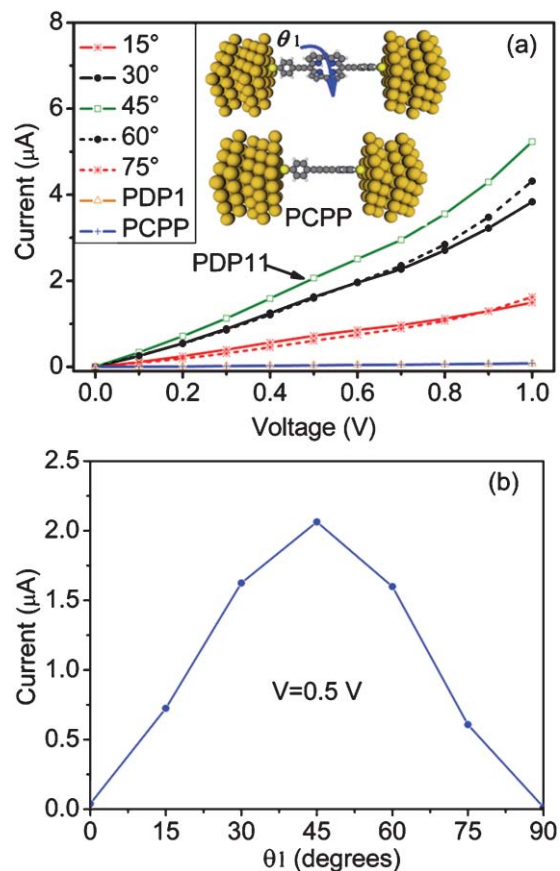


FIG. 8. (a) The  $I$ - $V$  curves for triad ethyne-bridged diphenyl porphyrin molecules with different torsion angles  $\theta_1$ . The two phenyls are always kept perpendicular to each other during the process. (b) The corresponding curve of current at 0.5 V versus  $\theta_1$  for the molecular junctions. The  $I$ - $V$  curves for PDP1 and PCPP junctions are also shown in (a).

#### IV. CONCLUSION

We have investigated the charge transport behaviors of different intramolecular conformations of ethyne-bridged phenyl porphyrin, phenyl porphyrin substituted with amino, phenyl porphyrin substituted with nitro, and diphenyl porphyrin molecules using an *ab initio* method, which is based on density function theory using norm conserving nonlocal pseudopotentials to define the atomic core and nonequilibrium Green's functions to calculate the charge distribution and electron transmission coefficients. The  $I$ - $V$  curves indicate that all these porphyrin-ethyne-benzene molecules can achieve a switching effect by regulating their intramolecular twist conformations. The reason is ascribed to the localization of the frontier molecular orbitals in real space in the molecular junctions containing any perpendicular structure between the parts of the circular conjugated molecules. Similar behavior was observed experimentally in electron transfer measurements.<sup>43,44</sup> The amino or nitro substitution close to the Au electrode can increase the ON/OFF ratio of ethyne-bridged phenyl porphyrin. We find that the substituents affect the entire molecules in coplanar conformation, but only local parts in perpendicular conformation, which causes switching with quite high efficiency being predicted in the case of nitro replacement. Multi-strategy switching behaviors are achieved

in ethyne-bridged diphenyl porphyrin molecules. Local overlap of the frontier molecular orbitals between the different parts in the wires determines the transmission of the junctions. In perpendicular conformations, the transmission of the junctions can be increased sensitively through effective super exchange interaction, by adding one more conjugated molecule with angles between neighbor  $\pi$  systems less than  $\pi/2$ . Conjugates or molecular wires constructed from conjugated planar cyclic groups, such as benzene, porphyrin, cyclopentadienyl, pyridine, etc., are all expected to present switching functions by controlling their intramolecular conformations. These findings could be useful to explain some experimental phenomena<sup>31</sup> and to choose or design molecular switching devices in the future molecular electronics.

#### ACKNOWLEDGMENTS

The work was supported by the National Natural Science Foundation of China (NNSFC) under Grant No. 10674027, 973-projects under Grant Nos. 2006CB921300 and 2011CB921803, the China Scholarship Council, Fudan High-end Computing Center, Beijing Computing Center, and by the ANSER Center, an Energy Frontier Research Center funded by the U.S. Department of Energy (DOE), Office of Science, Office of Basic Energy Sciences, under Award No. DE-SC0001059.

- <sup>1</sup>S. Datta, *Electronic Transport in Mesoscopic Systems* (Cambridge University Press, Cambridge, England, 1995).
- <sup>2</sup>M. Di Ventra, *Electrical Transport in Nanoscale Systems* (Cambridge University Press, Cambridge, England, 2008).
- <sup>3</sup>J. C. Cuevas and E. Scheer, *Molecular Electronics: An Introduction to Theory and Experiment*, (World Scientific, Singapore, 2010).
- <sup>4</sup>A. Pecchia and A. D. Carlo, *Rep. Prog. Phys.* **67**, 1497 (2004).
- <sup>5</sup>M. Brandbyge, J. L. Mozos, P. Ordejon, J. Taylor, and K. Stokbro, *Phys. Rev. B* **65**, 165401 (2002).
- <sup>6</sup>J. M. Soler, E. Artacho, J. D. Gale, A. García, J. Junquera, P. Ordejon, and D. Sánchez-Portal, *J. Phys.: Condens. Matter* **14**, 2745 (2002).
- <sup>7</sup>J. Taylor, H. Guo, and J. Wang, *Phys. Rev. B* **63**, 245407 (2001).
- <sup>8</sup>V. Mujica, A. Nitzan, Y. Mao, W. Davis, M. Kemp, A. Roitberg, and M. A. Ratner, *Adv. Chem. Phys.* **107**, 403 (1999).
- <sup>9</sup>J. A. Malen, S. K. Yee, A. Majumdar, and R. A. Segalman, *Chem. Phys. Lett.* **491**, 109 (2010).
- <sup>10</sup>N. J. Tao, *Nat. Nanotechnol.* **1**, 173 (2006).
- <sup>11</sup>K. H. Khoo, J. B. Neaton, Y. W. Son, M. L. Cohen, and S. G. Louie, *Nano Lett.* **8**, 2900 (2008).
- <sup>12</sup>W. Sheng, Z. Y. Ning, Z. Q. Yang, and H. Guo, *Nanotechnology* **21**, 385201 (2010).
- <sup>13</sup>K. Stokbro, J. Taylor, and M. Brandbyge, *J. Am. Chem. Soc.* **125**, 3674 (2003).
- <sup>14</sup>S. O. Koswatta, M. S. Lundstrom, and D. E. Nikonov, *Nano Lett.* **7**, 1160 (2007).
- <sup>15</sup>E. Lörtscher, J. W. Cizek, J. Tour, and H. Riel, *Small* **2**, 973 (2006).
- <sup>16</sup>F. Moresco, G. Meyer, K. H. Rieder, H. Tang, A. Gourdon, and C. Joachim, *Phys. Rev. Lett.* **86**, 672 (2001).
- <sup>17</sup>J. He, Q. Fu, S. Lindsay, J. W. Cizek, and J. M. Tour, *J. Am. Chem. Soc.* **128**, 14828 (2006).
- <sup>18</sup>M. Di Ventra, S. T. Pantelides, and N. D. Lang, *Phys. Rev. Lett.* **84**, 979 (2000).
- <sup>19</sup>P. Reddy, S. Y. Jang, R. A. Segalman, and A. Majumdar, *Science* **315**, 1568 (2007).
- <sup>20</sup>N. Wang, H. M. Liu, J. W. Zhao, Y. P. Cui, Z. Xu, Y. F. Ye, M. Kiguchi, and K. Murakoshi, *J. Phys. Chem. C* **113**, 7416 (2009).
- <sup>21</sup>S. U. Lee, R. V. Belosludov, H. Mizuseki, and Y. Kawazoe, *Small* **4**, 962 (2008).

- <sup>22</sup>P. Banerjee, D. Conkin, S. Nanayakkara, T. H. Park, M. J. Therien, and D. A. Bonnell, *ACS Nano* **4**, 1019 (2010).
- <sup>23</sup>L. Karki, F. W. Vance, J. T. Hupp, S. M. LeCours, and M. J. Therien, *J. Am. Chem. Soc.* **120**, 2606 (1998).
- <sup>24</sup>F. D. Angelis, S. Fantacci, A. Sgamellotti, M. Pizzotti, F. Tessore, and A. O. Biroli, *Chem. Phys. Lett.* **447**, 10 (2007).
- <sup>25</sup>A. W. Ghosh, T. Rakshit, and S. Datta, *Nano Lett.* **4**, 565 (2004).
- <sup>26</sup>C. B. Madsen, L. B. Madsen, S. S. Viftrup, M. P. Johansson, T. B. Poulsen, L. Holmegaard, V. Kumarappan, K. A. Jørgensen, and H. Stapelfeldt, *Phys. Rev. Lett.* **102**, 073007 (2009); *J. Chem. Phys.* **130**, 234310 (2009); S. Ramakrishna and T. Seideman, *Phys. Rev. Lett.* **99**, 103001 (2007).
- <sup>27</sup>G. Kresse and J. Furthmüller, *Phys. Rev. B* **54**, 11169 (1996).
- <sup>28</sup>C. C. Kaun and H. Guo, *Nano Lett.* **3**, 1521 (2003).
- <sup>29</sup>N. Troullier and J. L. Martins, *Phys. Rev. B* **43**, 1993 (1991).
- <sup>30</sup>M. Büttiker, Y. Imry, R. Landauer, and S. Pinhas, *Phys. Rev. B* **31**, 6207 (1985).
- <sup>31</sup>S. Lara-Avia, A. Danilov, V. Geskin, S. Bouzakraoui, S. Kubatkin, J. Cornil, and T. Bjørnholm, *J. Phys. Chem. C* **114**, 20686 (2010).
- <sup>32</sup>W. H. Wang, X. Q. Shi, M. C. Jin, C. Minot, M. A. Van Hove, J. P. Collin, and N. Lin, *ACS Nano* **4**, 4929 (2010).
- <sup>33</sup>W. F. Xiang and C. K. Lee, *Appl. Phys. Lett.* **96**, 193113 (2010).
- <sup>34</sup>A. S. Blum, J. G. Kushmerick, D. P. Long, C. H. Patterson, J. C. Yang, J. C. Henderson, Y. Yao, J. M. Tour, R. Shashidhar, and B. R. Ratna, *Nature Mater.* **4**, 167 (2006).
- <sup>35</sup>C. J. Xia, C. F. Fang, P. Zhao, S. J. Xie, and D. S. Liu, *Phys. Lett. A* **373**, 3787 (2009).
- <sup>36</sup>K. Stokbro, J. Taylor, M. Brandbyge, J. L. Mozos, and P. Ordejon, *Comput. Mater. Sci.* **27**, 151 (2003).
- <sup>37</sup>H. Basch, R. Cohen, and M. A. Ratner, *Nano Lett.* **5**, 1668 (2005).
- <sup>38</sup>J. R. Platt, *Free-Electron Theory of Conjugated Molecules* (University of Chicago, Chicago, 1964).
- <sup>39</sup>X. Y. Xiao, L. A. Nagahara, A. M. Rawlett, and N. J. Tao, *J. Am. Chem. Soc.* **127**, 9235 (2005).
- <sup>40</sup>S. Yeganeh, M. Galperin, and M. A. Ratner, *J. Am. Chem. Soc.* **129**, 13313 (2007).
- <sup>41</sup>M. A. Ratner *J. Phys. Chem.* **94**, 4877 (1990).
- <sup>42</sup>H. M. McConnell, *J. Chem. Phys.* **35**, 508 (1961).
- <sup>43</sup>A. Helms, D. Heiler, and G. McLendon, *J. Am. Chem. Soc.* **113**, 4325 (1991).
- <sup>44</sup>V. Loveras, J. Vidal-Gancedo, D. Ruiz-Molina, T. M. Figueira-Duarte, J. F. Nierengarten, J. Veciana, and C. Rovira, *Faraday Discuss.* **131**, 291 (2006).